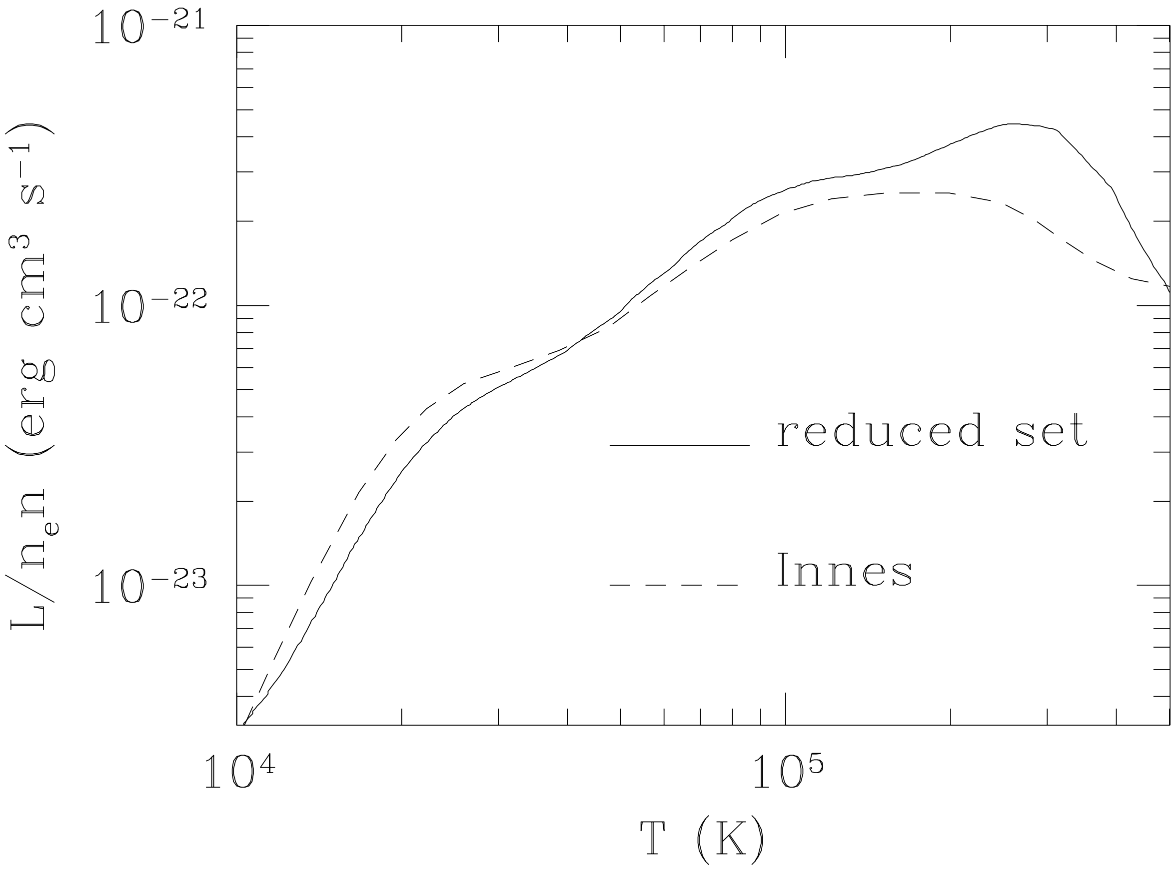

Fig. 1.— Time-dependent cooling function $L/n_e n$ (where L is the total cooling per unit volume and time, n_e is the electron density and n is the density of atoms and ions) for a parcel of constant density $n = 1$ cm^{-3} cooling from an initial temperature $T_1 = 10^6$ K. The solid curve shows the cooling function obtained from the "reduced set" of ionization rate equations described in the text. The dashed curve corresponds to the cooling function obtained from the considerably more detailed calculations of Innes (1985).

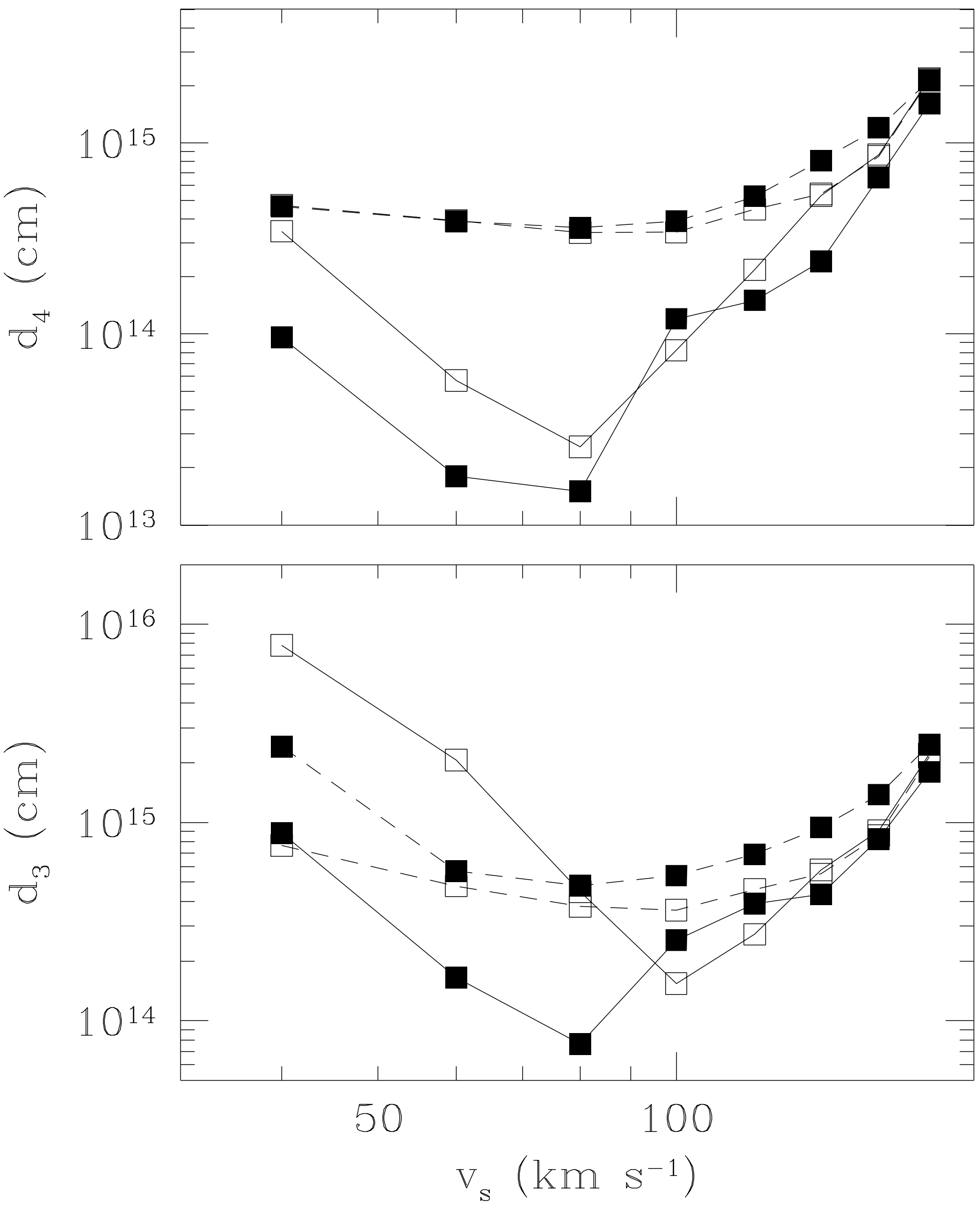

Fig. 2.— Cooling distances d_4 (top graph, corresponding to the distance between the shock and the point where a temperature of 10^4 K has been reached in the recombination region) and d_3 (bottom graph, corresponding to the distance where the post-shock gas has reached 10^3 K) as a function of shock velocity v_s for a grid of plane shock models with a pre-shock density $n_0 = 100$ cm^{-3}. The results from the models of Hartigan et al. (1987) are shown with filled squares, and the results from our simplified cooling models are shown with open squares. The dashed lines indicate models computed assuming that the pre-shock gas has fully ionized hydrogen. The solid lines indicate models that have been computed with "self-consistent preionization" (in the case of the models of Hartigan et al. 1987, solid squares) or models that have been computed assuming that the pre-shock hydrogen is neutral (in the case of our models, open squares).

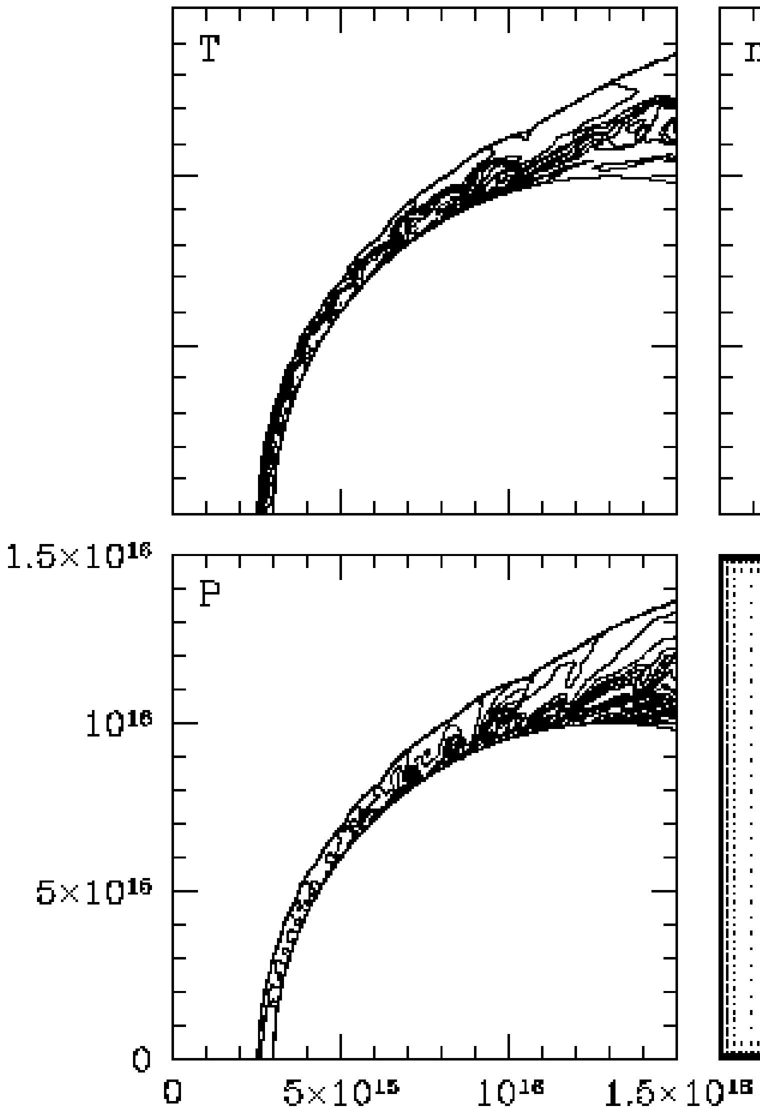

Fig. 3.— Results from the blunt body flow simulation described in the text. The temperature (top left), density (top right) and pressure (bottom left) stratifications are shown with logarithmic, $\sqrt{2}$ contours. The bottom left graph shows the distribution of grid points resulting from the adaptive, binary refining grid of the Coral code.

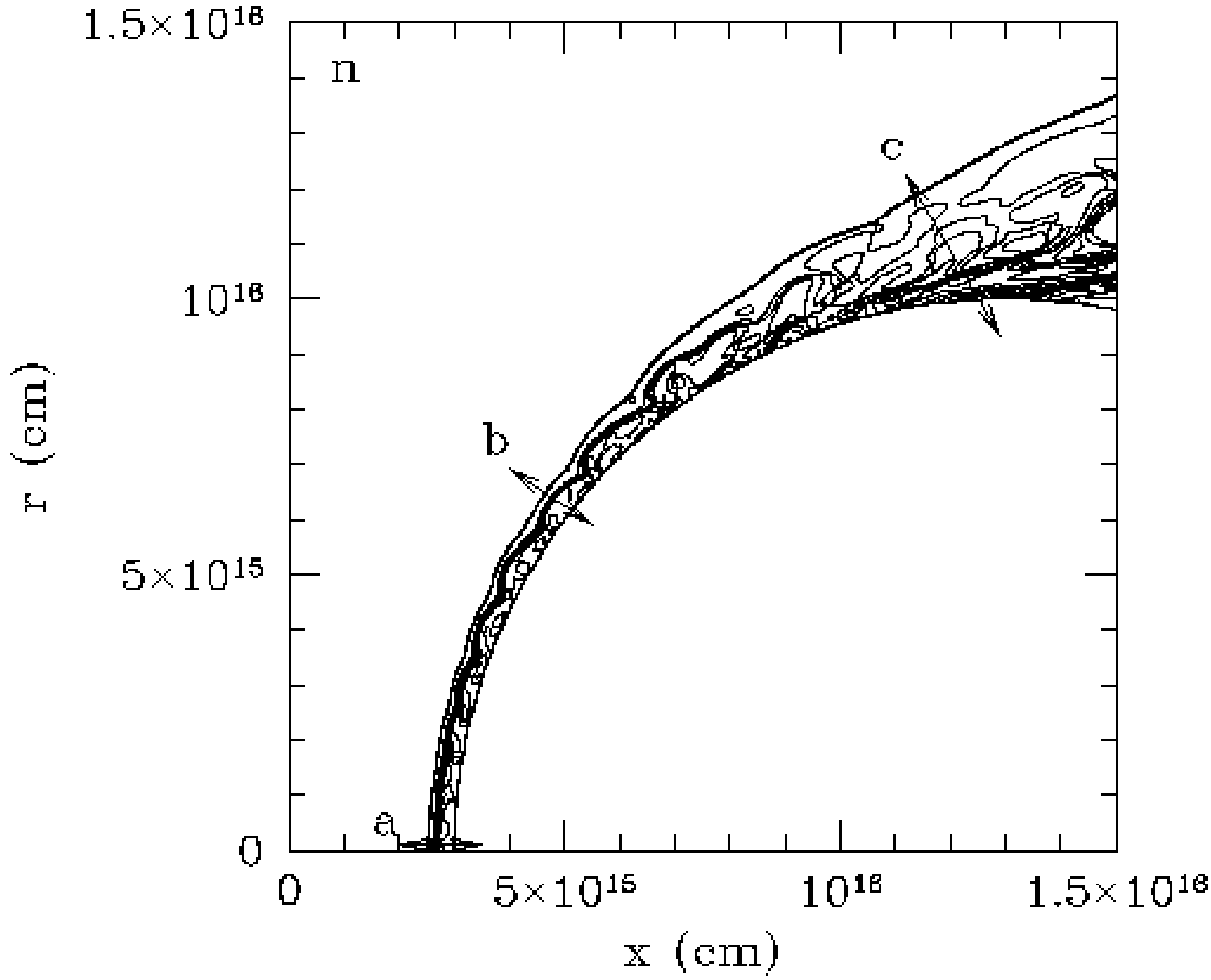

Fig. 4.— Diagram with the density distribution resulting from the blunt body flow simulation described in the text (with logarithmic, $\sqrt{2}$ contours). Superimposed on this diagram, we show three cuts (a, b and c) across the flow, all of them taken normal to the surface of the bow shock. Figures 5-10 show different flow variables measured along these cuts.

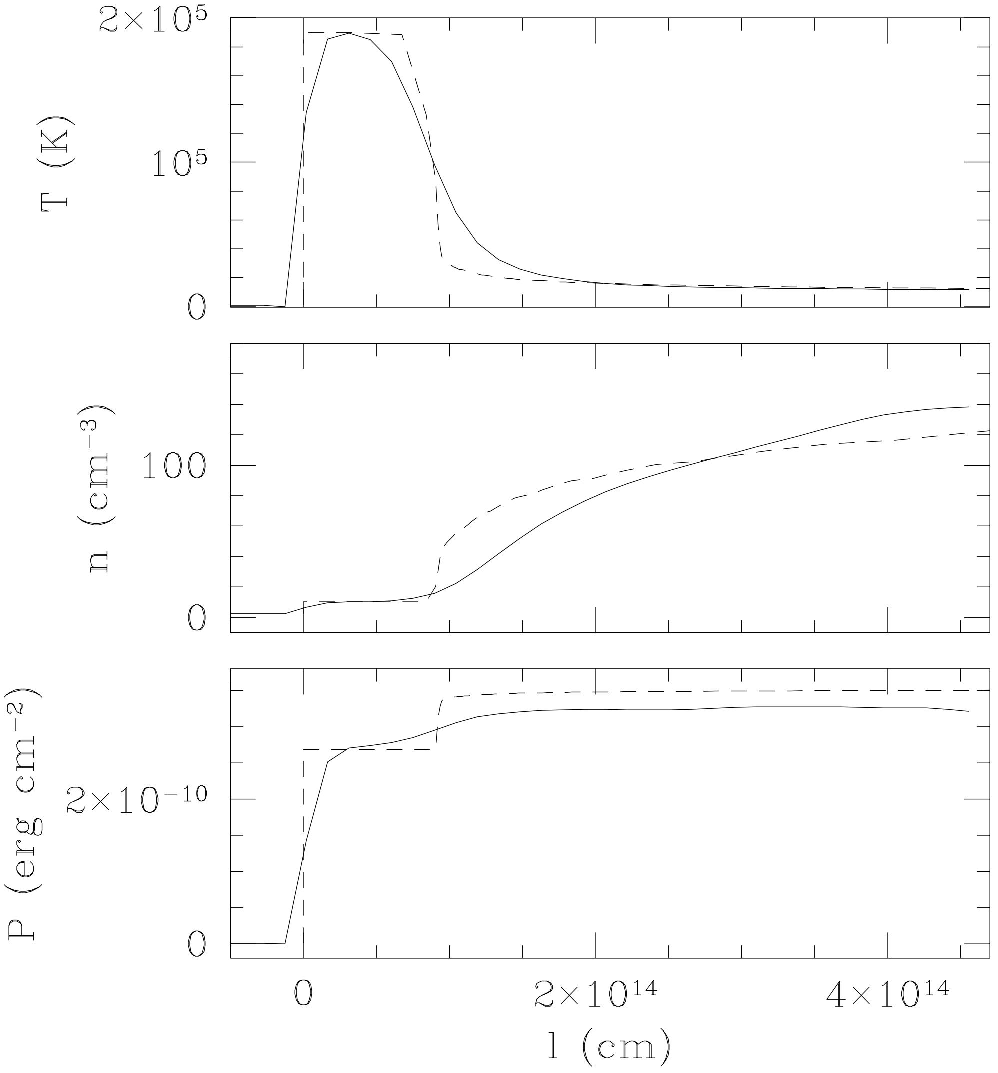

Fig. 5.— The temperature (top), ion+atom number density (center) and pressure (bottom) measured along cut a (see the text and Fig. 4) are shown with the solid lines. The ordinate l is defined so that $l = 0$ corresponds to the position of the bow shock. The x-axis of the graphs extends exactly to the position of the rigid body. Also shown in the graphs (with dashed lines) are the corresponding variables obtained from a steady, plane shock model of appropriate pre-shock parameters (see the text).

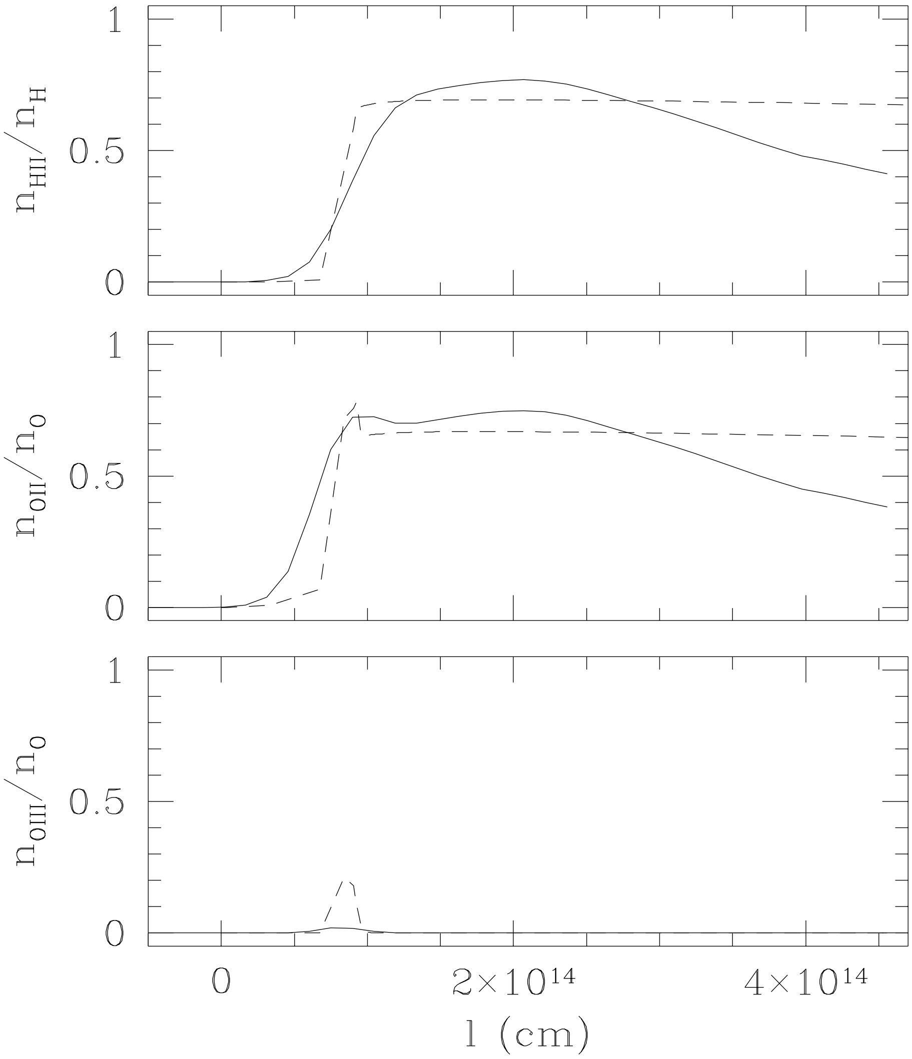

Fig. 6.— The hydrogen (top), O II (center) and O III (bottom) ionization fractions measured along cut *a* (see the text and Fig. 4). The solid lines show the results from the blunt body flow, and the dashed lines show the result from a steady, plane shock model of appropriate pre-shock parameters (see the text and also the caption of Fig. 5).

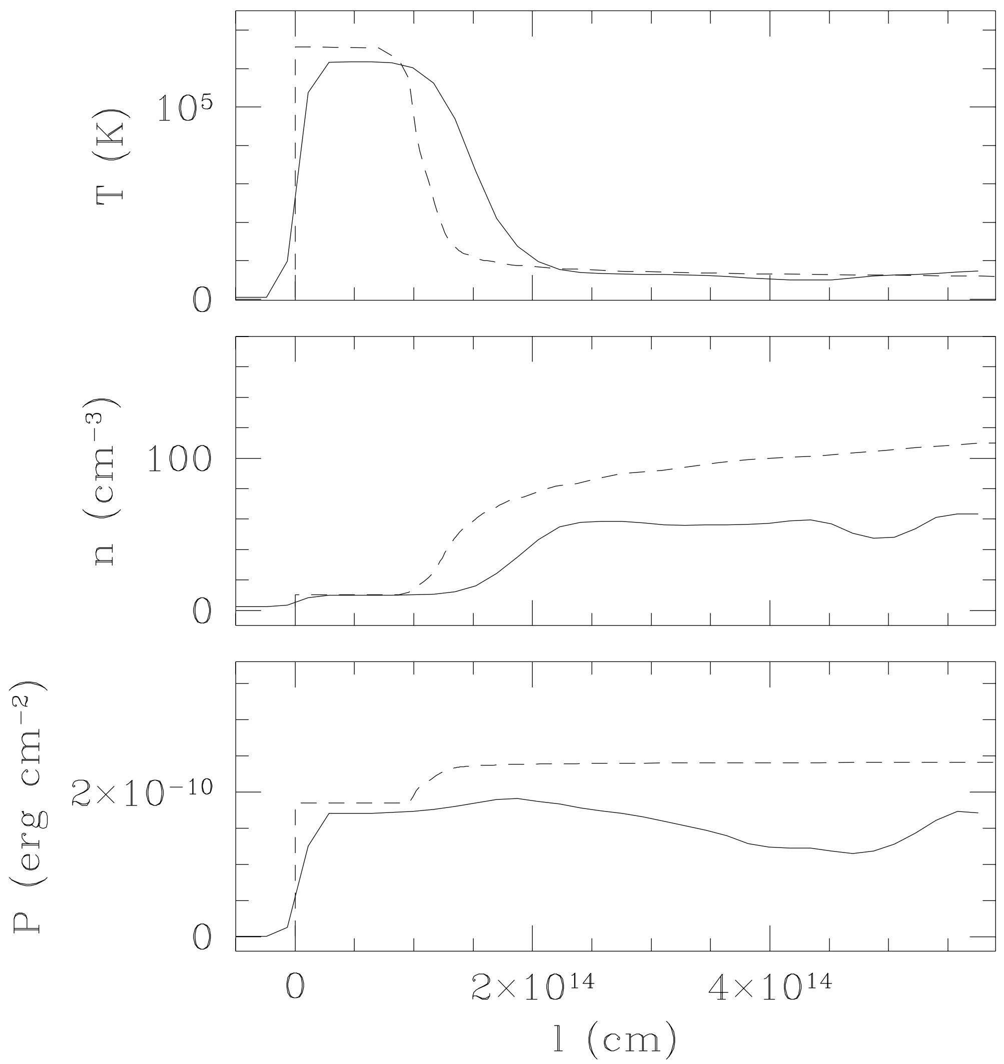

Fig. 7.— The temperature (top), ion+atom number density (center) and pressure (bottom) measured along cut *b* (see the text and Fig. 4). The solid lines show the results from the blunt body flow, and the dashed lines show the result from a setady, plane shock model of appropriate pre-shock parameters (see the text and also the caption of Fig. 5).

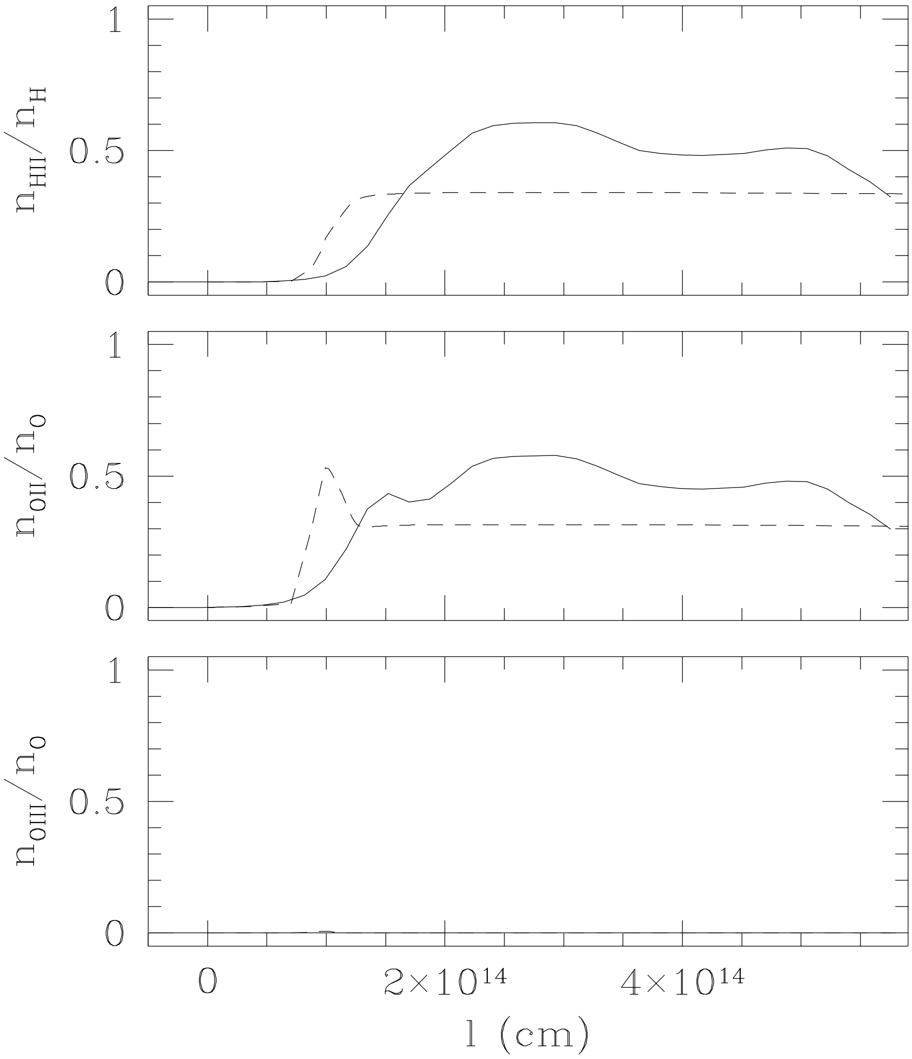

Fig. 8.— The hydrogen (top), O II (center) and O III (bottom) ionization fractions measured along cut *b* (see the text and Fig. 4). The solid lines show the results from the blunt body flow, and the dashed lines show the result from a steady, plane shock model of appropriate pre-shock parameters (see the text and also the caption of Fig. 5).

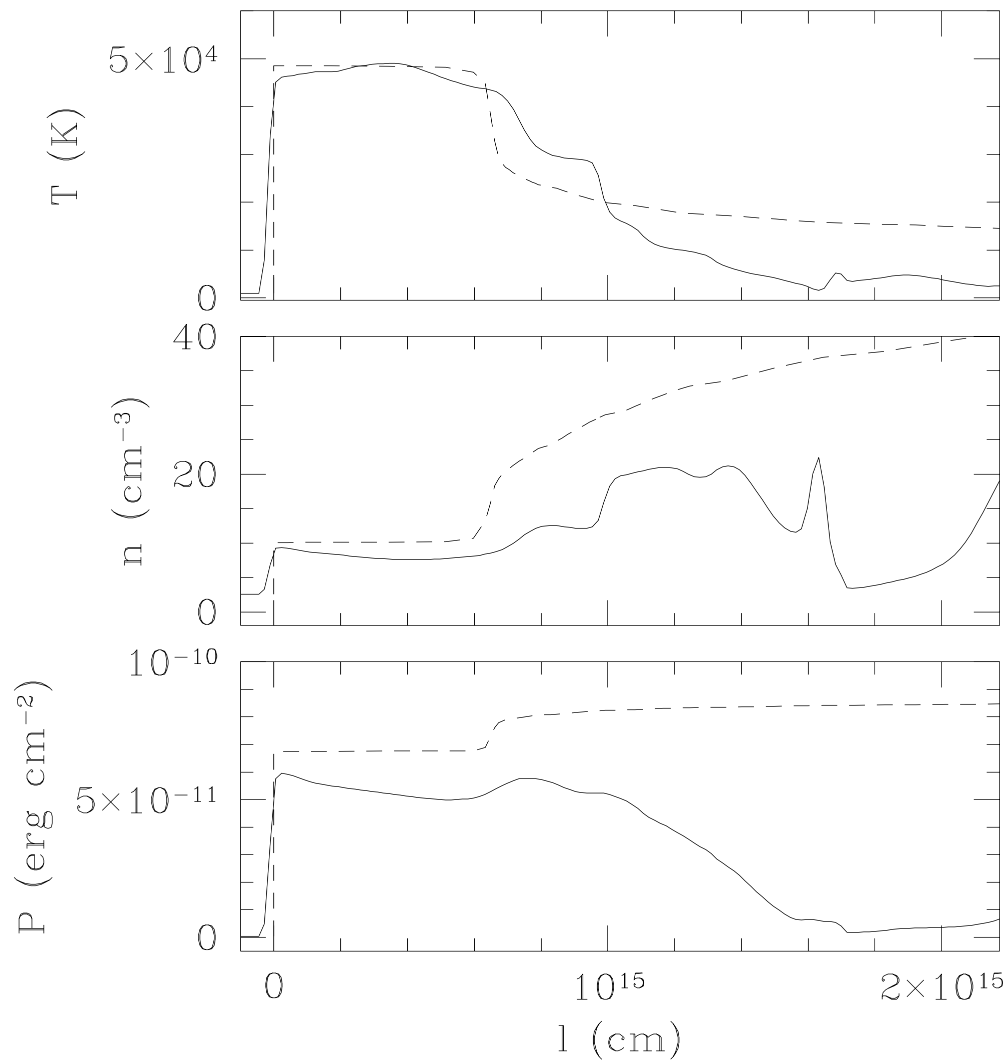

Fig. 9.— The temperature (top), ion+atom number density (center) and pressure (bottom) measured along cut c (see the text and Fig. 4). The solid lines show the results from the blunt body flow, and the dashed lines show the result from a steady, plane shock model of appropriate pre-shock parameters (see the text and also the caption of Fig. 5).

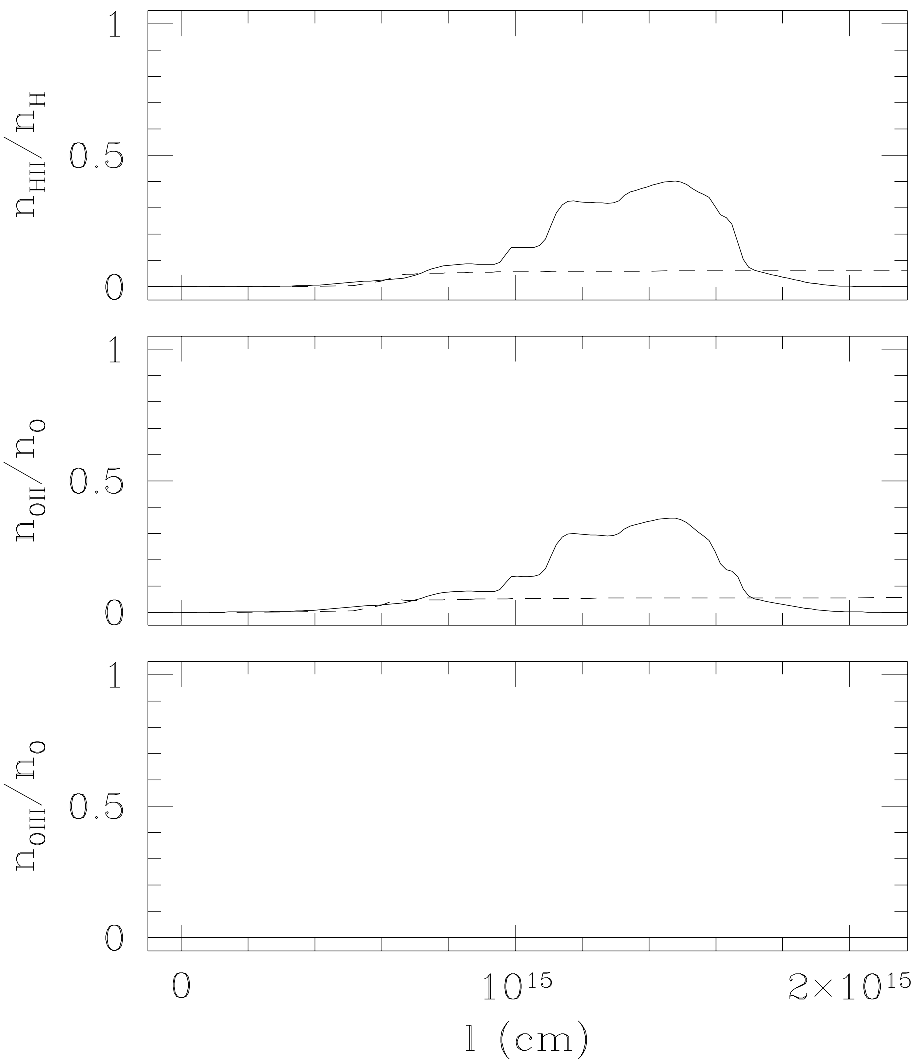

Fig. 10.— The hydrogen (top), O II (center) and O III (bottom) ionization fractions measured along cut c (see the text and Fig. 4). The solid lines show the results from the blunt body flow, and the dashed lines show the result from a steady, plane shock model of appropriate pre-shock parameters (see the text and also the caption of Fig. 5).